

Safety-relevant V2X beaconing in realistic and scalable heterogeneous radio propagation fading channels

Daniel Bischoff^{1,2}, Harald Berninger¹, Steffen Knapp¹, Tobias Meuser², Björn Richerzhagen², Lars Häring³ and Andreas Czylik³

¹Active Safety Advanced Technology, Opel Automobile GmbH, Rüsselsheim, Germany

²Multimedia Communication, Technische Universität Darmstadt, Darmstadt, Germany

³Telecommunication Systems, Universität Duisburg-Essen, Duisburg, Germany

{[daniel.bischoff](mailto:daniel.bischoff@opel.com), [steffen.knapp](mailto:steffen.knapp@opel.com)}@opel.com, harald.berninger@gmx.de, {[tobias.meuser](mailto:tobias.meuser@kom.tu-darmstadt.de), [bjorn.richerzhagen](mailto:bjorn.richerzhagen@kom.tu-darmstadt.de)}@kom.tu-darmstadt.de, {[haering](mailto:haering@nts.uni-duisburg-essen.de), [czylik](mailto:czylik@nts.uni-duisburg-essen.de)}@nts.uni-duisburg-essen.de

Keywords: Heterogeneous Communication, V2X, 802.11p, LTE, Geocast, Channel Gain, Channel Load.

Abstract: Performance evaluations for heterogeneous communication technologies in the area of V2X safety applications for either improvement, comparison or combination purposes are in general focusing on the realistic representation of the upper communication stack layers, but therefore - often for the sake of simplicity - reducing the radio propagation channel to a maximum range model. The impact and hence the importance to model the environment dependent propagation effects in a representative manner has already been stressed in the literature several times - but separately for ad-hoc or cellular systems and not under the consideration of V2X safety-beaconing applications. By combining a realistic heterogeneous radio propagation channel model with a state-of-the-art V2X communication stack, a representative performance comparison of safety-relevant beaconing applications for 802.11p single-hop broadcast (SHB) and LTE Geocast can be conducted. Our simulation results show that the effects caused by the radio propagation channel cannot be neglected as they significantly impact key communication performance metrics such as channel gain, packet error ratio (PER) and channel load, where we primarily focus on the latter one to give further research directions for an efficient dissemination of safety-relevant V2X beacons.

1 INTRODUCTION

Safety-relevant V2X applications aim at improving safety and efficiency on the road by exchanging information such as vehicle dynamic or traffic data between vehicles and the infrastructure. To enable vehicular communications, IEEE 802.11p and 3GPP LTE are the most promising communication technologies, which are recently in the focus of performance evaluations (Araniti et al., 2013), where the former is following an ad-hoc and the latter a cellular approach. To identify the performance of vehicular communications and especially to compare the aforementioned communication technologies, several metrics have been derived to address the individual needs of V2X safety applications. Such metrics mainly focus on reliability, channel load, coverage and latency (Xiao et al., 2019).

Radio propagation channels in vehicular communication systems are subject to severe fading caused by the high mobility and rich scattering environ-

ment (Bernado et al., 2014). Shadowing by other vehicles and the infrastructure (large-scale fading) and multipath propagation causing delay and Doppler spread (small-scale fading) impact the packet reception power and therefore the packet error ratio (PER) at the receiver (Viriyasitavat et al., 2015) significantly. Even though there are plenty of channel models mentioned in the literature, almost all performance evaluation studies currently use very simplified radio propagation channel models for ad-hoc communication or assume an error-free communication for cellular communication. These simplified channel models reduce the complexity of radio propagation effects to a maximum transmission range model, similar to (Guenther et al., 2016), to reduce the computational complexity of the simulation. Although, especially in motorway environments, it was shown that fading effects impact the reliability of the communication and therefore have to be considered in the radio propagation channel model (Bernado et al., 2014).

In this paper, we propose a realistic and scalable het-

erogeneous channel model, which foremost follows a simplified geometry-based deterministic (GBD) approach to consider path loss, large- and small-scale fading effects for both radio technologies using a heterogeneous channel model. This approach differentiates us from existing V2X performance evaluation studies, where different and simplified or non-scalable channel models are used for each radio communication technology. By that, we improve the comparison between both technologies, where we also consider the individual propagation characteristics, such as multipath propagation for each technology. As a result of the high mobility of vehicles, V2X safety applications require a frequent and continuous exchange of information (beaconing) to improve the localization of other vehicles. We show that the choice of the channel model can severely impact the simulation results of the channel load for 802.11p. To support long-range dissemination in V2X communication systems, cellular systems such as LTE are in the focus to support V2X safety-applications (Araniti et al., 2013). Cellular systems are usually not suited to support beaconing applications, especially if a unicast transmission is considered in the downlink (Vinel, 2012). In contrast to that, multicast transmission can significantly reduce the channel load in the downlink but requires a multicast session setup prior to the message dissemination, which can take up to seconds (Araniti et al., 2013). We analyze the ability of LTE Geocast using unicast transmission mode to support V2X beaconing applications and compare the channel utilization for both communication technologies using our heterogeneous channel model. Therefore, our main contributions of this paper are:

- Realistic and scalable heterogeneous V2X radio propagation channel model
- Comparison of LTE and 802.11p channel gain and PER with high vehicle density using a realistic heterogeneous channel model
- Impact of channel models on the channel load for 802.11p SHB V2X beaconing applications and comparison with LTE Geocast dissemination

The rest of this paper is organized as follows: In Section 2 we summarize the related work of V2X channel models and performance evaluations. In Section 3 we introduce our proposed heterogeneous channel model and the message dissemination mechanisms for both communication technologies. The simulation setup is briefly summarized in Section 4. We evaluate our channel model in Section 5 and compare the channel load with both communication technologies. The paper will be concluded in Section 6.

2 RELATED WORK

In this section, we briefly introduce the related work for V2X channel models and V2X performance evaluations.

2.1 V2X Channel Model

Radio propagation effects can be grouped into two main categories, that is, path loss propagation, large-scale and small-scale fading. To model these effects, we can use GBD, geometry-based stochastic (GBS) or non-geometry based stochastic (NGS) approaches. The following channel models obtain stochastic parameters from measurement campaigns in different environments and therefore fit in the area of NGS approaches: For V2V communications, free-space propagation has been addressed in (Nilsson et al., 2017), large-scale fading in (Boban et al., 2011) and small-scale fading in (Acosta-Marum and Ingram, 2007) and (Bernado et al., 2014) separately for different environments such as urban and suburban areas as well as motorways. A comprehensive survey on V2X channel models has been conducted in (Viriyasitavat et al., 2015). In (Maaz et al., 2015), a V2I path loss measurement has been conducted for an urban environment.

In GBS approaches, the representation of fading is still achieved stochastically, but takes the environment into account. In (Czink and Oestges, 2008), based on the geometry of the environment, the authors define three types of different clusters, group reflectors and scatterers as clusters and parametrize them in accordance to the number of reflectors and scatterers within the respective cluster. Finally, small-scale fading is stochastically modeled for each cluster. The *Winner* channel model (Kysti et al., 2008) also describes small-scale fading with the help of clusters. These stochastic models also rely on empiric data obtained from measurement campaigns and are not available for every frequency spectrum and scenario.

GBD models usually do not rely on measurement campaign datasets to model propagation effects of the communication channel. In (J. Maurer and T. Fugen and T. Schafer and W. Wiesbeck, 2004) the authors propose a ray-tracing approach to determine large- and small-scale fading effects. The authors showed that the accuracy is very high when comparing it to measurement campaigns within the same scenario. Neglecting multipath propagation, the authors in (Boban et al., 2011) modeled the large-scale fading in a simplified deterministic manner. Here, only the direct link between the transmitter and receiver is considered. Even though there are plenty of

channel models available, the related work currently misses a realistic and scalable channel model, which describes the radio propagation effects for different communication technologies in a similar way. By doing this, the comparisons of different communication technologies is increased, and we can evaluate large-scale scenarios.

2.2 V2X Performance Evaluation

To analyze the ability to support vehicular communications for different radio technologies, several performance comparisons have been conducted. In (Hameed Mir and Filali, 2014), the authors compared the throughput, End-to-End Latency, and Packet Delivery Ratio (PDR) for LTE and 802.11p, using a Log-Distance and Nakagami fading model. In (Moller et al., 2014), the authors considered a very detailed ray-tracing channel model to describe the radio propagation effects in a deterministic manner. Nevertheless, the evaluation was limited to the PDR and Block Error Ratio (BLER). The performance of the Decentralized Congestion Control (DCC) for 802.11p and its impact on the channel load was extensively studied in (Guenther et al., 2016), where a maximum range channel model was used. In (Cecchini et al., 2017), the resource allocation for LTE-D2D was studied using a path loss channel mode. A comprehensive survey on the comparison of V2X communication technology can be found in (Masini et al., 2018). To the best of our knowledge, simulations to obtain the performance for V2X safety beaconing applications under realistic radio propagation channel conditions for the aforementioned performance metrics in a heterogeneous communication environment (cellular and ad-hoc) has not been conducted yet.

3 SYSTEM DESIGN

In this section, we derive our realistic and scalable heterogeneous channel model. Furthermore, we explain the message dissemination strategy for LTE and 802.11p, that is, Geocast and SHB, respectively.

3.1 Design of the heterogeneous Channel Model

Figure 1 depicts the complete structure of the channel model, where we determine the communication link, path loss, large-scale fading and small-scale fading separately. In summary, our channel model aims at obtaining a realistic and scalable representation of

radio propagation effects for 802.11p and LTE in vehicular communication systems.

The output is the time-invariant channel impulse response $h(t, \tau)$. In the simulator $h(t, \tau)$ is calculated at the receiver for each vehicle separately and the absolute square of $h(t, \tau)$ is mapped with the transmission signal power. The level of the resulting reception power is used to determine if the message can be decoded correctly.

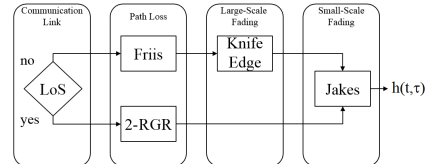


Figure 1: Structure of the V2X channel model.

3.1.1 Communication Link

With the help of the geometry of objects in the simulation environment, antenna heights of both transmitter and receiver and the first *Fresnel Ellipsoid*, the condition of the communication link can be obtained, that is, Line-Of-Sight (LOS) or Non-Line-Of-Sight (NLOS). In (Boban et al., 2011) LOS is expected, if 60% of the first *Fresnel Ellipsoid* is free of obstacles. We assume the same for our model. We make use of the implementation in (Sommer et al., 2015), where the authors implemented the shadowing model described in (Boban et al., 2011). We extend this approach to obtain the LTE link condition as well. We use the link condition information to increase the accuracy of path loss and large-scale fading, as requested in (Nilsson et al., 2017) and (Boban et al., 2011), respectively.

3.1.2 Path Loss

The free-space path loss is often modeled with the *Friis* equation, which only holds under idealistic environment conditions. The benefit of this model is its generality, that is, the variable use of different carrier frequencies, thus making it easy to use different communication technologies working in different spectra. The *Friis* formula is given in Equation 1, where λ and d denote the carrier wavelength and the distance between the transmitter and receiver, respectively. P_T , P_R , G_T and G_R denote the transmission and reception power as well as the transmitter and receiver antenna gain, respectively.

$$\frac{P_R}{P_T} = \left(\frac{\lambda}{2\pi d} \right)^2 \cdot G_R \cdot G_T \quad (1)$$

Under the condition of LOS, the two-ray ground reflection model (2-RGR) is used. The superposition of the direct and reflected wave at the receiver cannot be ignored, as detailed in (Nilsson et al., 2017). The relationship between received and transmitted power is given in Equation 2, where h_T and h_R denote the antenna height at the transmitter and receiver, respectively.

$$\frac{P_R}{P_T} = \left(\frac{\lambda}{2\pi d} \right)^2 \cdot \left(2 \sin \left(\frac{2\pi}{\lambda} \cdot \frac{h_T h_R}{d} \right) \right)^2 \cdot G_R \cdot G_T \quad (2)$$

3.1.3 Large-Scale Fading

Depending on the propagation path of the radio wave, there is a probability that objects, such as buildings or other vehicles, shadow the path of the propagation wave. The resulting attenuation can be described with the single (in case of one object) or multiple-knife edge model (in case of more than one object) as detailed in (Boban et al., 2011).

Besides the calculation of large-scale fading attenuation for 802.11p, we extend the implementation in (Sommer et al., 2015) to obtain the attenuation caused by large-scale fading effects for the LTE channel model in (Viridis et al., 2015). Our implementation considers the carrier frequency and antenna heights of the respective communication technology.

3.1.4 Small-Scale Fading

Fast amplitude fluctuation of the received signal is caused by constructive and destructive superposition of multiple waves (multi-path propagation) at the receiver antenna. The incoming waves are shifted in time and frequency due to Doppler effect and time delay of each wave. In (Viridis et al., 2015), a modified Jakes model (Jakes, 1974) is used, which simplifies the calculation of multi-path propagation. This approach differentiates between mobile nodes and base stations and assumes a fixed amount of waves with a random angle of arrival for the mobile nodes and the same angle of arrival for the base stations. The propagation delay of each fading path at the receiver is normally distributed with the root-mean-square (RMS) delay spread as requested in (Jakes, 1974). The relative speed of vehicles is retrieved from the microscopic traffic simulator SUMO (Krajzewicz et al., 2002), to calculate the respective phase shift of each wave (Doppler effect), obtain the total phase shift (Doppler and Delay spread) and hence determine the channel impulse response $h(t, \tau)$.

3.1.5 Scalability

The calculation of path loss and small-scale fading in our proposed channel model do not depend on other objects. Hence, the computational complexity per V2X-enabled vehicle is mainly affected by the determination of the communication link. As only the direct path between receiver and transmitter is considered, the computational complexity per node is $O(V + I)$, where V and I depict the number of vehicles and the number of other interfering objects such as buildings and infrastructures, respectively. In contrast to that, ray-tracing approaches, as described in (J. Maurer and T. Fugen and T. Schafer and W. Wiesbeck, 2004), tend to have a computational complexity greater than $O((V + I)^2)$ (Viriyasitavat et al., 2015) per node and therefore cannot be considered for large-scale simulations.

3.2 Message Dissemination

For 802.11p, we consider a simple SHB dissemination as beacons are usually addressed to the immediate surrounding of the vehicle.

For LTE, we use unicast transmission mode in both up- and downlink directions in order to obtain results for a worst-case scenario in terms of channel load. This also avoids time-expensive session setups for multicast transmission. We implement the Geocast mechanism described in (Intelligent Transport Systems, 2012). The simulation area is divided in cells, where each cell will be encoded into a Geohash (Niemeyer, 2008). When a vehicle leaves its current cell, it will send a location update to the GeoServer. The GeoServer calculates the new Geohash and sends the boundaries of the next cell back to the respective vehicle. Hence, the GeoServer is able to forward beacons to all vehicles within the same cell (Geohash) of the transmitter.

4 SIMULATION SETUP

In this section, we describe our simulation setup.

4.1 Simulator

The representation of the map scenario and traffic flow is realized using SUMO 0.32 (Krajzewicz et al., 2002), which is connected by the TraCI interface to the communication simulator Veins 4.7 (Sommer et al., 2011), representing the 802.11p stack. Veins builds on OMNeT++ 5.3 (Varga and Hornig, 2008). The LTE stack is implemented in SimuLTE, which

was modified in (Virdis et al., 2015) to work in V2X network simulations. The simulation parameters are listed in Table 1. The RMS delay spreads for 802.11p and LTE microscopic simulations were taken from (Bernado et al., 2014) and (Virdis et al., 2015), respectively.

4.2 Scenario Design

For the simulation scenario, a motorway intersection at the Frankfurter Kreuz in Germany was chosen, where the selected section was extracted from OpenStreetMap (FOSSGIS e.V., 2018) and converted to a SUMO compatible format. The resulting map file is depicted in Figure 2. For the evaluation of the channel load for 802.11p, a network probe (Probe) is installed in the center of the Frankfurter Kreuz. The maximum interference range is set to 1500 m, as this distance is in the order of the maximum theoretical transmission range following Equation 1 under the assumption of the transmission power, antenna gain and sensitivity from Table 1. For cellular LTE communications, two base stations, one at the Frankfurter Kreuz (eNB1) and another one to the south of the A5 (eNB2), are assumed and connected via a X2 connection to enable handovers. The locations and antenna heights of both base stations were taken from (Bundesnetzagentur, 2016). The size of the map area covers the communication range for two base stations. The scenario

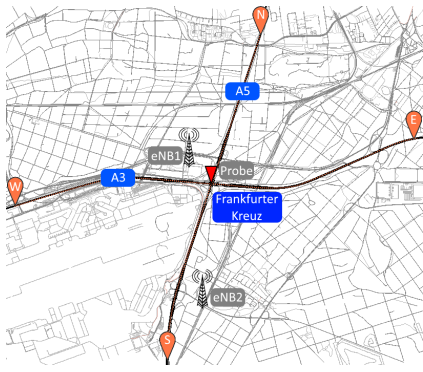


Figure 2: Motorway scenario: *Frankfurter Kreuz* in SUMO (Krajzewicz et al., 2002).

is characterized by its high traffic density and high relative velocities. The former is taken from the BAST database in 2016¹ (Kraftfahrt Bundesamt, 2016), such that the motorway is populated as follows:

- A3: 4692 vehicles and 985 trucks driving from the west (W) to the east (E) side and 4950 vehicles and 860 trucks in the opposite direction per hour

¹The maximum traffic density within the whole year was taken

- A5: 7933 vehicles and 776 trucks from the north (N) to the south side (S) and 5988 vehicles and 796 trucks in the opposite direction per hour and driving direction

During the simulation run, vehicles and trucks were driving with a mean velocity of 126 km/h and 96 km/h, where the maximum allowed velocity was set to 180 km/h and 100 km/h, respectively.

5 EVALUATION

In order to show the characteristics of the heterogeneous channel model, we evaluate the channel gain and PER for both radio technologies. As the main contribution of this paper, we also evaluate the channel load for both radio technologies under the consideration of a realistic heterogeneous channel model, using a safety-relevant V2X beaconing application.

We briefly summarize our performance metrics, which will be later used in the evaluation. The *Channel Gain* describes the environment dependent attenuation of the signal in dB, when traveling from the transmitter to the receiver. The antenna gains on both sides are not considered, as we are interested in the radio propagation channel effects. *Packet Error Ratio* is the number of packets which cannot be decoded correctly at the receiver side, denoted by $N_{p,err}$, divided by the number of all received packets, denoted by $N_{p,suc}$. Hence, the PER is $N_{p,err}/N_{p,suc}$. For our evaluation, we obtain the PER in distance bins with a length of 10 m and 50 m for 802.11p and LTE, respectively. We determine the median as well as the lower and upper quartile for distance bins of length 100 m and 500 m for 802.11p and LTE, respectively, derived from the smaller distance bins described before. The *Channel Load* describes the ratio of the capacity used to the theoretical maximum capacity. The available channel bandwidth physically limits the channel capacity. For 802.11p, we use the Channel Busy Ratio (CBR) as the performance metric for the channel load, which was also used in (Guenther et al., 2016). For LTE, we obtain the cell block utilization for both bands in the up- and downlink, which is supported by the LTE scheduler in (Virdis et al., 2015).

5.1 Channel Gain

5.1.1 802.11p

The measurement results are obtained from all vehicles within the simulation time and are depicted in Figure 3. The channel gain measurements depicted in blue and black indicate the condition of LOS and

Table 1: Overview of the simulation parameters.

General		802.11p		LTE	
Simulation time	100..120 s	Carrier frequency	5.89 GHz	Carrier frequency	2 GHz
Map Area	33.8 km ²	Channel bandwidth	10 MHz	Channel bandwidth	10 MHz
Beacon size	300 B	Bit rate	6 Mb/s	Coding rate	AMC
Beacon Interval	10 Hz	Transmit Power	21 dBm	Transmit Power (eNB)	46 dBm
Thermal noise	-104.5 dBm	Sensitivity	-89.5 dBm	Number of Bands (up/down)	2
Fading paths	6	Antenna Gain	3 dB	Antenna Gain (Vehicle)	3 dB
Antenna height cars	1.5 m	Interference range	1500 m	Antenna Gain (eNB)	16 dB
Antenna height trucks	2.4 m	Transmit Mode	SHB	Transmit Mode	Unicast
Antenna height (eNB1)	27 m	Delay spread RMS	0.644 μ s	Delay spread RMS	0.363 μ s
Antenna height (eNB2)	25.4 m			Geohash length	7

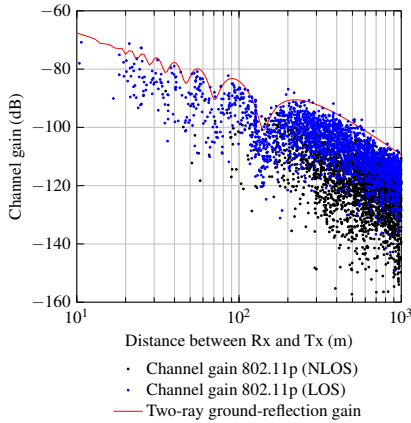


Figure 3: Channel Gain over distance for 802.11p.

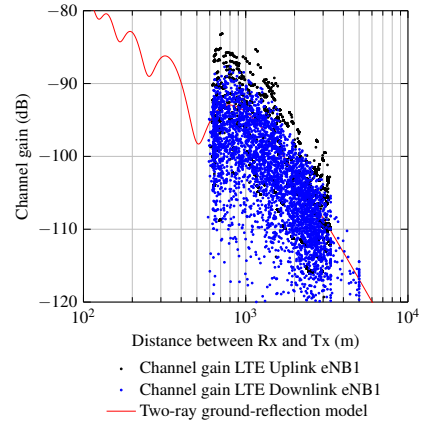


Figure 4: Channel Gain over distance for LTE.

NLOS, respectively. The upper limit of the channel gain (LOS, blue) is bounded by the 2-RGR, where the ideal 2-RGR is depicted in red, following the attenuation term of Equation 2. The lower limit of the channel gain is unbounded due to fading (NLOS, black). The channel gain fluctuation is increased at larger distances as the probability of an obstruction in the propagation path is increased. We validated our proposed model with measurement results obtained in a motorway scenario from (Nilsson et al., 2017). Within the distance bins of 10 m, 100 m and 1000 m, the channel gain differs in the order of 3 dB, 5 dB and 2 dB, respectively.

5.1.2 LTE

The channel gain for LTE in the downlink (blue) and uplink (black) channel from eNodeB1 (eNB1) is depicted in Figure 4. The channel gain follows the 2-RGR model. As the antenna at the base station is at the height of 27 m, the LOS link is dominant, even though we consider mixed traffic in our simulation environment. The fluctuation of the channel gain is caused by the Jakes fading model, where constructive and destructive interference appears. The representation of the channel gain is different in the up- and

downlink channel, that is, the Jakes fading model differentiates between both communication directions. The recent literature currently lacks real-world measurements for V2X LTE channel gain in different environments and frequency spectra. In (Maaz et al., 2015), the path loss in the downlink was measured at 2.1 GHz in an urban environment and differentiates between LOS and NLOS condition. Unfortunately, there are no measurement results available for LOS condition between a distance of 500 m and 3000 m. In comparison with our channel model, the lower limit of the channel gain for NLOS is roughly 20 dB higher compared to our results. This is justified by the high attenuation due to shadowing in urban scenarios.

5.2 Packet Error Ratio

For both radio technologies, the PERs are depicted in Figure 5. For 802.11p the PER increases with distance and at 1000 m almost no packet can be decoded correctly. The PER for LTE in the up- and downlink is significantly lower. The median PER is below 0.05 and 0.03 in the up- and downlink, respectively. In contrast to 802.11p, where the code and hence the bit rate is not adapting to the condition of the radio prop-

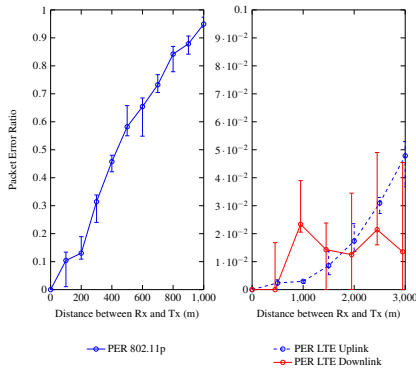


Figure 5: PER for 802.11p and LTE (Up- and Downlink).

agation channel, LTE can leverage from the feedback channel. We compared our results with real-world measurements in a suburban scenario from (Liu et al., 2016). The PER for LTE up to a distance of 500 m is almost 0%, which is in accordance with our measured PER (below 1% at 500 m distance). The PER for 802.11p is at 30% and 45% at a distance of 300 m and 500 m, respectively. This is also in accordance with our results, where we obtained a PER of 25% and 45% for the aforementioned distance bins.

5.3 Channel Load

Finally, we analyse the impact of beacons on the channel load for ad-hoc and cellular communication using our realistic radio propagation channel model. In Figure 6, the channel load is represented as CBR for 802.11p and cell block utilization for LTE.

The box plot to the left depicts the CBR for the realistic channel model (Realistic) proposed in Section 2.1 and the maximum range channel model (Range) for 802.11p, where the maximum transmission range is set to 300 m. The median of the CBR for the realistic channel model is roughly 0.17 compared to 0.1 for the maximum range channel model. Maximum range channel models neglect all packets above the maximum transmission range. This assumption reduces the local CBR for each vehicle, as only packets within a radius of 300 m are received. In contrast to that, the realistic channel model still receives a certain amount of packets up to a distance of 1000 m as depicted in Figure 5, which increases the total number of locally received packets for each vehicle. We showed, that radio propagation channel models significantly impact the representation of the channel load for microscopic simulations.

On the right side of Figure 6, the cell block utilization for LTE enB1 in the up- and downlink is depicted. The downlink channel is completely saturated as depicted in Figure 6. As we use unicast transmission

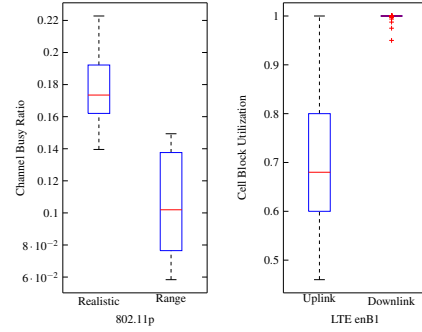


Figure 6: Channel load for 802.11p (realistic and range channel model) and LTE (Up- and Downlink).

mode in the downlink channel, each beacon has to be forwarded to each member of the same cell separately, which increases the cell load. The cell block utilization is lower in the uplink, where the median is around 0.68. This also indicates that the uplink channel is saturated by more than 2/3 of the total bandwidth (10 MHz) used in the simulation, even without considering channel usage by other devices such as mobile phones.

6 CONCLUSION

Performance evaluations in the context of microscopic V2X heterogeneous communication systems are often dramatically simplifying the radio propagation channel to a maximum transmission range model. In this paper, we investigated a realistic heterogeneous radio propagation channel model for large-scale simulations with respect to the computational complexity. We presented first measurement results for ad-hoc and cellular communication using a beaconing application in a highly populated motorway scenario to obtain results for channel gain, PER and channel load.

In our evaluation, we showed that the channel model significantly impacts the CBR for 802.11p. We compared our results with a maximum range transmission model, which was frequently used in the literature. Furthermore, we shed light on the channel load for LTE Geocast. Even though we choose the cell size to be small, the channel load was high in the uplink and saturated in the downlink. We also showed that the channel load for V2X beaconing applications was lower for 802.11p compared to LTE.

In our future work, we plan to investigate advanced dissemination strategies and filter rules to extend the LTE Geocast approach. Furthermore, we use heterogeneous communication systems to improve the dissemination of safety-relevant V2X messages.

REFERENCES

- Acosta-Marum, G. and Ingram, M. A. (2007). Six time- and frequency- selective empirical channel models for vehicular wireless LANs. *IEEE Vehicular Technology Magazine*, 2(4):4–11.
- Araniti, G., Campolo, C., Condoluci, M., Iera, A., and Molinaro, A. (2013). LTE for vehicular networking: a survey. *IEEE Communications Magazine*, 51(5).
- Bernado, L., Zemen, T., Tufvesson, F., Molisch, A. F., and Mecklenbrucker, C. F. (2014). Delay and Doppler Spreads of Nonstationary Vehicular Channels for Safety-Relevant Scenarios. *IEEE Transactions on Vehicular Technology*, 63(1):82–93.
- Boban, M., Vinhoza, T. T. V., Ferreira, M., Barros, J., and Tonguz, O. K. (2011). Impact of Vehicles as Obstacles in Vehicular Ad Hoc Networks. *IEEE Journal on Selected Areas in Communications*, 29(1):15–28.
- Bundesnetzagentur (2016). EMF-Datenbank. <https://emf3.bundesnetzagentur.de/karte/>. Last checked on Dec 14, 2018.
- Cecchini, G., Bazzi, A., Masini, B. M., and Zanella, A. (2017). LTEV2Vsim: An LTE-V2V simulator for the investigation of resource allocation for cooperative awareness. In *2017 5th IEEE International Conference on Models and Technologies for Intelligent Transportation Systems (MT-ITS)*, pages 80–85.
- Czink, N. and Oestges, C. (2008). The COST 273 MIMO Channel Model: Three Kinds of Clusters. In *2008 IEEE 10th International Symposium on Spread Spectrum Techniques and Applications*, pages 282–286.
- FOSSGIS e.V. (2018). OpenStreetMap - Deutschland. <https://www.openstreetmap.de/>. Last checked on Dec 14, 2018.
- Guenther, H. J., Riebl, R., Wolf, L., and Facchi, C. (2016). Collective perception and decentralized congestion control in vehicular ad-hoc networks. In *2016 IEEE Vehicular Networking Conference (VNC)*, pages 1–8.
- Hameed Mir, Z. and Filali, F. (2014). LTE and IEEE 802.11p for vehicular networking: a performance evaluation. *EURASIP Journal on Wireless Communications and Networking*, 2014(1):89.
- Intelligent Transport Systems (2012). Framework for Public Mobile Networks in Cooperative ITS (C-ITS). Technical report, ETSI.
- J. Maurer and T. Fugen and T. Schafer and W. Wiesbeck (2004). A new inter-vehicle communications (IVC) channel model. In *IEEE 60th Vehicular Technology Conference, 2004. VTC2004-Fall. 2004*, volume 1.
- Jakes, W. C. (1974). *Microwave Mobile Communications*. John Wiley & Sons.
- Kraftfahrt Bundesamt (2016). Fahrzeugbestand im Ueberblick. <https://www.kba.de/DE/Statistik/>. Last checked on Apr 14, 2018.
- Krajzewicz, D., Hertkorn, G., Roessel, C., and Wagner, P. (2002). SUMO (Simulation of Urban MOBility); An open-source traffic simulation. *4th Middle east symposium on simulation and modelling (MESM 2002)*.
- Kysti, P., Meiril, J., and Hentil, L. (2008). Winner II Channel Models ver. 1.2. Technical Report D1.1.2, Winner II Project.
- Liu, Z., Liu, Z., Meng, Z., Yang, X., Pu, L., and Zhang, L. (2016). Implementation and performance measurement of a V2X communication system for vehicle and pedestrian safety. *International Journal of Distributed Sensor Networks*, 12(9):1550147716671267.
- Maaz, I., Conrat, J., and Cousin, J. (2015). Channel Model Validation for the Relay-Mobile Link in Microcell Environment. In *2015 IEEE 82nd Vehicular Technology Conference (VTC2015-Fall)*, pages 1–5.
- Masini, B., Bazzi, A., and Zanella, A. (2018). A survey on the roadmap to mandate on board connectivity and enable V2V-based vehicular sensor networks. *Sensors*, 18(7):2207.
- Moller, A., Nuckelt, J., Rose, D. M., and Kurner, T. (2014). Physical Layer Performance Comparison of LTE and IEEE 802.11p for Vehicular Communication in an Urban NLOS Scenario. In *2014 IEEE 80th Vehicular Technology Conference (VTC2014-Fall)*, pages 1–5.
- Niemeyer, G. (2008). Geohash. <https://en.wikipedia.org/wiki/Geohash>. Last checked on Dec 14, 2018.
- Nilsson, M. G., Gustafson, C., Abbas, T., and Tufvesson, F. (2017). A Measurement-Based Multilink Shadowing Model for V2V Network Simulations of Highway Scenarios. *IEEE Transactions on Vehicular Technology*, 66(10):8632–8643.
- Sommer, C., German, R., and Dressler, F. (2011). Bidirectionally Coupled Network and Road Traffic Simulation for Improved IVC Analysis. *IEEE Transactions on Mobile Computing*, 10(1):3–15.
- Sommer, C., Joerer, S., Segata, M., Tonguz, O. K., Lo Cigno, R., and Dressler, F. (2015). How Shadowing Hurts Vehicular Communications and How Dynamic Beacons Can Help. *IEEE Transactions on Mobile Computing*, 14(7):1411–1421.
- Varga, A. and Hornig, R. (2008). An Overview of the OM-NeT++ Simulation Environment. In *Proceedings of the 1st International Conference on Simulation Tools and Techniques for Communications, Networks and Systems & Workshops*.
- Vinel, A. (2012). 3GPP LTE Versus IEEE 802.11p/WAVE: Which Technology is Able to Support Cooperative Vehicular Safety Applications? *IEEE Wireless Communications Letters*, 1(2):125–128.
- Viridis, A., Stea, G., and Nardini, G. (2015). Simulating LTE/LTE-Advanced Networks with SimuLTE. In *Simulation and Modeling Methodologies, Technologies and Applications*.
- Viriyasitavat, W., Boban, M., Tsai, H., and Vasilakos, A. (2015). Vehicular Communications: Survey and Challenges of Channel and Propagation Models. *IEEE Vehicular Technology Magazine*, 10(2):55–66.
- Xiao, L., Zhuang, W., Zhou, S., and Chen, C. (2019). *Intelligent Network Access System for Vehicular Real-Time Service Provisioning*, chapter Intelligent Network Access System for Vehicular Real-Time Service Provisioning, pages 79–104. Springer International Publishing, Cham.